Materials Science and Engineering A 417 (2006) 134–142

www.elsevier.com/locate/msea

Segregation substructures in dilute Al–Cu alloys directionally solidified

Osvaldo Fornaro[1,*], Hugo A. Palacio[2], Heraldo Biloni[2]

Instituto de Física de Materiales Tandil (IFIMAT), Universidad Nacional del Centro de la Provincia de Buenos Aires, Pinto 399, B7000GHG Tandil, Argentina

Received in revised form 12 October 2005; accepted 1 November 2005

Abstract

Directional growth of dilute Al–0.2 wt.% Cu alloy was performed under conditions of controlled solidification. Proper metallographic analysis of the segregation patterns behind the solid–liquid (S–L) interface gives information about the effect of the local solidification conditions that determines the microsegregation. In order to explain the apparition of different solidification substructure as a function of the parameter (G_L/VC_0) (G_L, thermal gradient in the liquid in front of the S–L interface; V, solidification rate and C_0, nominal composition of the alloy), as well as the small segregated instabilities detected at the cellular walls, a mechanism based on the morphological stability theory is proposed.

PACS: 81.30.Fb; 45.70.Qj

Keywords: Directional solidification; Morphological stability; Cellular growth; Microsegregation

1. Introduction

In the directional solidification of dilute alloys, the morphological stability theory [1–3] defines the conditions under which a planar solid–liquid (S–L) interface becames unstable. According to this theory, at low and moderate solidification rates, modified constitutional supercooling (MCS) criteria can be applied and the classical expression of Tiller et al. [4] can be considered valid [5] when the thermal conductivities in the solid and the liquid phase κ_L and κ_S are similar. As a result, from a qualitative point of view, the decrease of the parameter

$$\frac{G_L}{VC_0} = \frac{m_L}{D_L}\,\frac{(k_0-1)}{k_0} \tag{1}$$

controls the evolution of the S–L interface from planar to arrayed dendritic. In this equation, m_L is the slope from the liquidus line from the phase diagram of the alloy, D_L is the liquid solute diffusion constant and k_0 is the partition coefficient under equilibrium conditions.

Extensive research has been done on this subject both in organic transparent alloys, in 2D symmetry, as well as in dilute alloys, giving information in a 3D symmetry. In the last case, the following stages may be defined [6] (i) planar S–L interface; (ii) nodes or depressions at the S–L interface; (iii) elongated or bi-dimensional cells; (iv) regular or hexagonal cells; (v) distorted or branched cells; (vi) dendritic cells or arrayed dendrites. Considering the technological importance of f.c.c. alloys as well as our experimental experience, the present work is concerned with Al–Cu dilute alloys. The current knowledge is unclear in connection with the mechanism involved in the evolution of the different stages. In the literature only some concepts exist such as a node mechanism [7,6], different expressions for the transition from the stage (v) to (vi) [8–10] and theoretical works concerned with the formation of the discrete stages (ii), (iii) and (iv) without discussion of the transition among them [11–13].

Upon review, the segregation details of the intercellular solute distribution were analyzed in some detail. A more careful metallographic analysis in dilute Al–Cu alloys that have been directionally grown may contribute to two important areas of understanding: (i) the segregation pattern of directional grown samples with different operational conditions (G_L/VC_0), and (ii) the possible mechanisms associated with the transitions among substructure stages above mentioned.

The fundamental aim of this work is to evaluate the details of the microsegregation substructure and to obtain a relationship between the pattern and the morphological evolution of the substructure during the directional solidification in dilute Al–

* Corresponding author.
E-mail address: ofornaro@exa.unicen.edu.ar (O. Fornaro).
[1] Consejo Nacional de Investigaciones Científicas y Técnicas.
[2] Comisión de Investigaciones Científicas de la Provincia de Buenos Aires.

0921-5093/$ – see front matter © 2005 Elsevier B.V. All rights reserved.
doi:10.1016/j.msea.2005.11.013

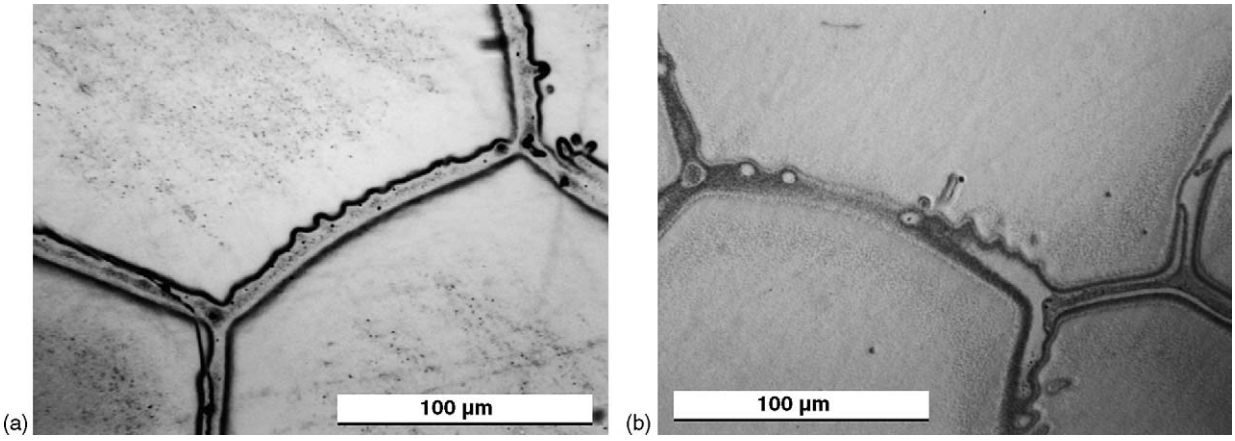

Fig. 1. Lateral perturbations in cellular growth. Samples grown at $G_L = 25$ K/cm. (a) $V = 12$ μm/s; at 2.5 mm far from the interface quenched; (b) $V = 13$ μm/s; sample without quench.

0.2 wt.% Cu alloys, presenting substructures that correspond to stages (ii) to (v), using proper metallographic techniques able to detect the details of the segregation substructure.

2. Experimental

Directional solidification of Al–0.2 wt.% Cu was carried out. The details of alloy preparation, growth of the samples, control of thermal and S–L interface velocity variables (G_L/VC_0), and quenching of the S–L interface during the growth can be found in the literature [14–17]. Usually, the samples were grown for several centimeters long and then, the interface was frozen with an axial flux of water, but some samples were obtained without the quenching process to compare the resulting structure.

The analysis of the microstructure requires great attention on the preparation of the samples. The microstructure was observed both in longitudinal views (in direction of the growth) and in cross sections. The surface was set up by mechanical polishing with up to 600 grit SiC abrasive paper and then with 6–1 μm diamond powder. Electrolytical polishing with 80 mL 2-butoxy-ethanol; 10 mL glycerine; 10 mL $HClO_4$ and aluminum cathode using a 33 V tension source during 15–60 s gives us an adequate surface in order to obtain a good contrast at high magnification. To reveal and emphasize the microstructure, the electropolished surfaces were etched using a solution of 20 mL HCl, 5 mL HNO_3, 2 mL HFl in 190 mL distilled water. This solution affects selectively rich copper zones, such as Al–Cu eutectics or solute rich zones with different relief. The etchant was diluted at 33% to slow down the reaction in some cases. The etching time was around 20 s at room temperature.

3. Results

It is well known that from a qualitative point of view, for a given alloy composition with $k_0 < 1$, an unstable planar growth evolves to a substructure where solute rich zones (nodes) correspond to depressions at the S–L interface as the (G_L/VC_0) parameter decreases. Even for a very low nominal composition, the concentration of the nodes can often grow up until it reaches the eutectic composition [18,19].

In this work, the evolution of the segregation substructure from stage (ii) (nodes) to stage (v) (irregular cells) was studied experimentally. We observed that in this broad range, the substructure presents a common characteristic: eutectic nodes isolated in stage (ii) joined by segregated undulated walls during the subsequent stages under study. This characteristic has been found in cross sections of the samples grown at low and moderate solidification rates. Fig. 1a corresponds to the intercellular microsegregation at near 2.5 mm down the quenched interface. The micrograph corresponds to a transversal cut of a cellular growth, taken near the quenched interface. In order to disregard the presumption that the metallographically observed segregation pattern could be promoted by rapid final solidification of liquid during the S–L interface quenching, the microstructure was observed at different distances from the quenched interface as well as in samples grown by several centimeters in

Table 1
Experimental data obtained in our experiences for Al–0.2 wt.% Cu and $G_L = 25$ K/cm

	V(μm/s)	λ_1 (μm)	λ_{min} (μm)
Nodes	5.5	369	24
	5.5	337	28
	5.5	271	24
	5.5	261	35.4
	5.5	280	27
	5.5	318	30
Bands	10	241	16.5
	12	269	14.1
	15	252	16.4
Cells	12	259	15.5
	13	193	12.6
	14	235	13.2
	14.5	247	14.1
	15	213	12.4
Irregular Cells	15	262	11.7
	16	287	11.9
	17	232	12.6
	20	195	12.6
	24	157	12.0
	27	160	10.3

length, typically 10 cm, and obtained without the S–L interface quenching process. Fig. 1b shows a microsegregated pattern in a sample without quenching, which is quite similar to Fig. 1a. It is clear that the lateral instabilities is a general phenomenon that may be interpreted as existent during the solidification process.

By increasing the growth velocity under the same thermal gradient and nominal composition, decreasing values of (G_L/VC_0) are obtained. Fig. 2a–j shows a sequence of micrographs obtained for a given value of G_L (25 K/cm) and increasing values of V. Fig. 2a shows eutectic nodes (stage (ii)), some of them connected by microsegregated areas. Fig. 2b shows a detailed zone between two adjacent nodes. These interconnections correspond to depressions of the S–L interface enriched in solute but without reaching the eutectic composition. Fig. 2c corresponds to the formation of two dimensional cells (stage (iii)) where the walls present different concentration areas, as well as lateral instabilities in some regions. Depressed zones with a greater eutectic precipitation are more evident, as in Fig. 2d. Fig. 2e and f show a banded structure close to achieving a regular cellular

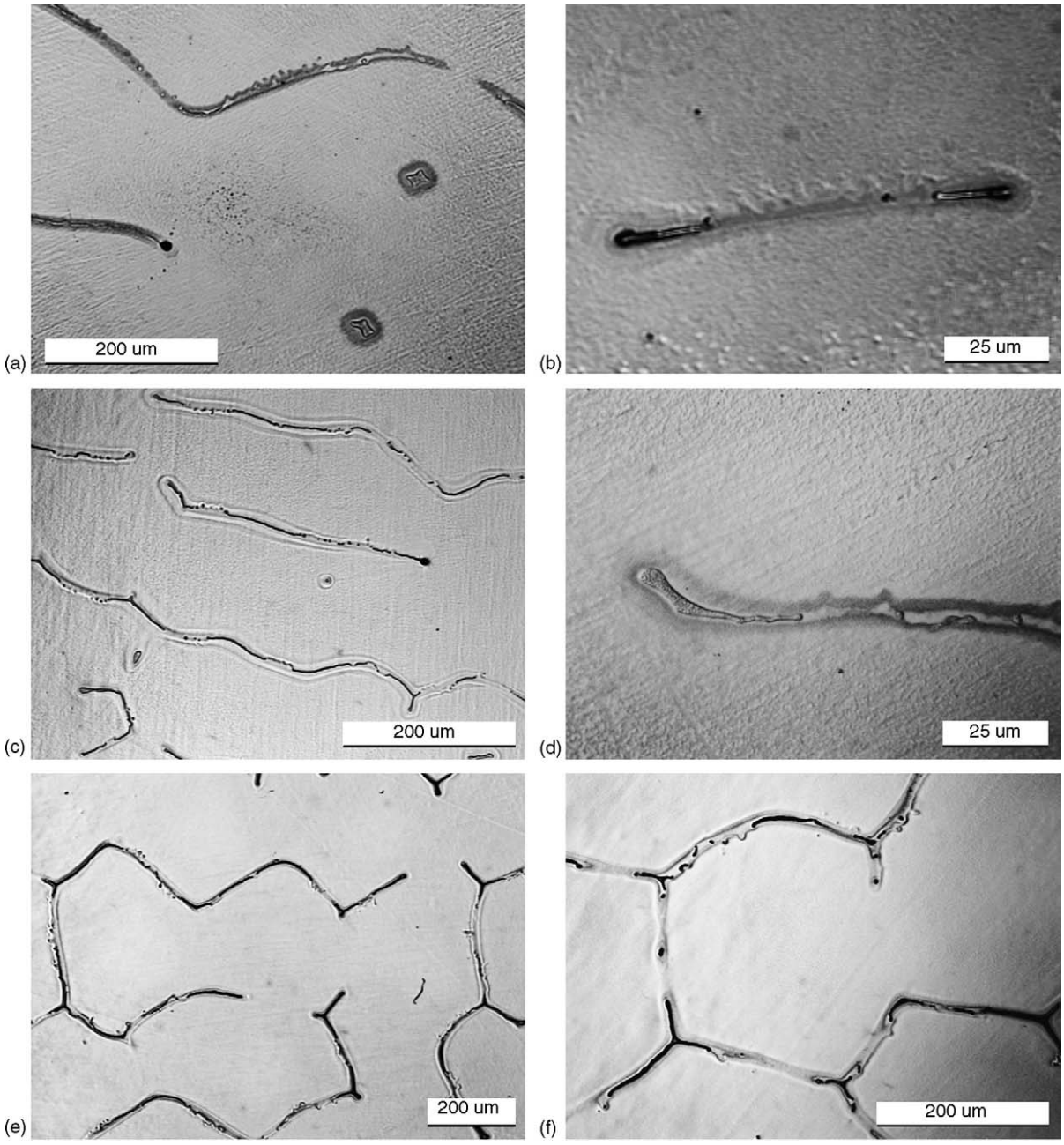

Fig. 2. Transversal view of Al–0.2 wt.% Cu for $G_L = 25$ K/cm and increasing V: (a) interconnected nodes, $V = 5.2$ μm/s and (b) detailed view of interconnected nodes; (c) bands at $V = 11$ μm/s and (d) detailed view of a wall where local perturbations exist; (e) bi-dimensional cells, $V = 11$ μm/s and (f) proto-cell, $V = 12$ μm/s. (g) hexagonal regular cell, $V = 13$ μm/s and (h) detail of a vertex node showing microsegregated pattern at cellular wall at high magnification; (i) irregular cell, at $V = 21$ μm/s cm/s and (j) amplified view of a cellular wall in an irregular cell stage. It is possible to observe undulations on both sides of the same wall in (c), (d) and (j).

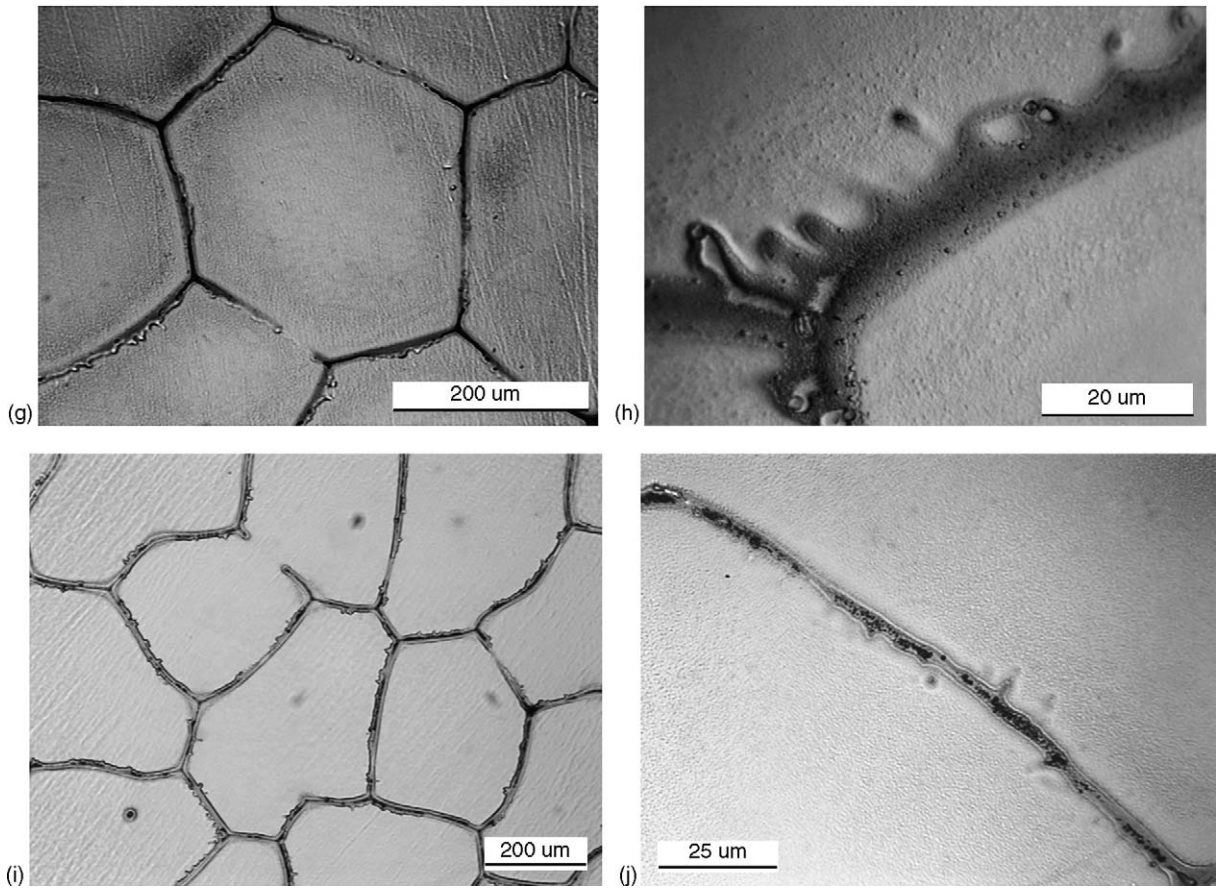

Fig. 2. (*Continued*).

pattern. Fig. 2e shows the transition between stages (iii) and (iv). The corners of the hexagons show a second phase precipitation that acts to pin future cell walls. This precipitation seems to be the θ-phase, which forms the eutectic with the adjacent Al α-phase. Fig. 2g shows a regular shaped cell. It can be seen that at cellular wall among nodes, the lateral growth presents lateral instabilities when the solute concentration is not enough to reach eutectic composition. Fig. 2h is a micrograph of a wall at high magnification, where a node at vertex and lateral instabilities can be shown. Notice, again, a similar variation of the composition, as observed before, in all the range analyzed. Finally, Fig. 2i shows a typical irregular substructure (stage (v)), having the same characteristic microstructure, and Fig. 2j a detailed zone of the substructure during stage (v).

A similar situation can be seen in longitudinal views of the samples as V is increased. Fig. 3a corresponds to cellular growth, stage (iv). At the segregated intercellular spacing a rippled segregation appears regularly. As in Fig. 2, in many cases, the wall was smooth from one side and perturbed from another, see Fig. 3b. As V is increased, this becomes more visible, as in Fig. 3c. The same picture shows that the lateral growth promotes nodal eutectic precipitation with a well determined spacing. These nodes correspond to the eutectic nodes revealed in cross section (Fig. 2).

The wavelengths of the observed perturbations were measured, revealing two kinds of characteristic spacing: a primary spacing λ_1, corresponding to the distance among eutectic nodes with a value between 150–300 μm and a dispersion of $\pm$4%, and a smaller segregated perturbation of the structure at the walls, which we call λ_{min}, taken as the distance between successive relative maximums in the perturbed walls, with a range between 15–25 μm and a typical dispersion of $\pm$8%. Both λ_1 and λ_{min} decrease as growth velocity increases, with a similar dependence. In Table 1, experimental λ_1 and λ_{min} values extracted from the experiments are given. It was possible to define a constant relationship between both perturbations as $\lambda_1/\lambda_{min} \approx 12$ for stages (ii) to (v) studied in this work.

4. Discussion

From the results shown in the sequence of Fig. 2a–j, corresponding to the evolution from stages (ii) to (v), a quite clear picture of the microsegregation features is obtained. This is an important fact from the technological point of view, due to the influence that microsegregation substructures, even at very low composition of solute, has on physical and chemical properties of cast samples [20]. We consider worthwhile speculating on the origin of λ_1 and λ_{min} using the current morphological theory.

During the directional solidification of dilute alloys, a planar unstable front can evolve to a cellular front, trapping solute in the intercellular space during the process. The mechanisms that define the spacing selection are under discussion. However, the fact

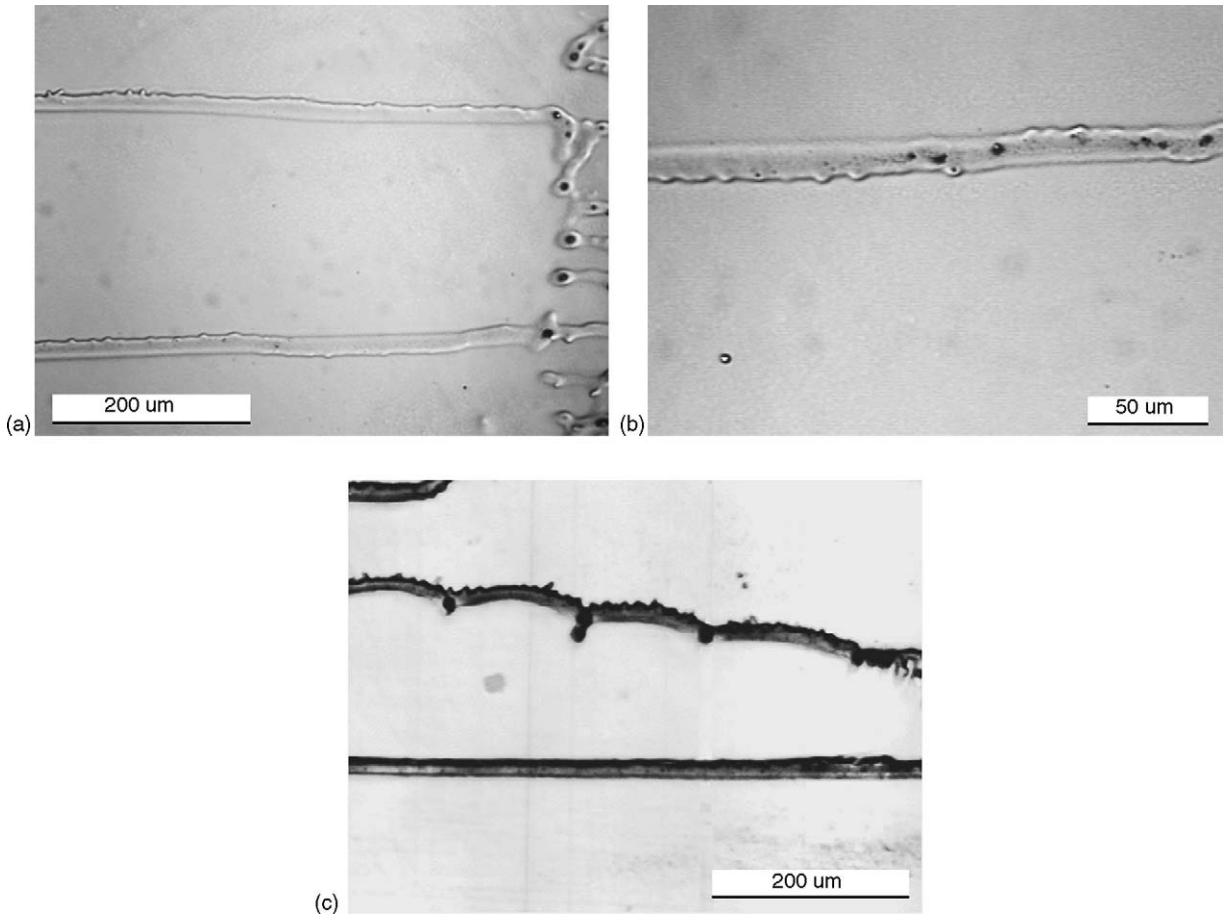

Fig. 3. Longitudinal view of Al–0.2 wt.% Cu for $G_L = 25$ K/cm, and increasing V. The growth is from right to left: (a) Lateral instabilities during cellular growth, $V = 12$ μm/s; (b) detailed view showing typical lateral perturbations in both sides of the cellular growth. $V = 12$ μm/s; (c) lateral growth promotes nodal precipitation, $V = 13$ μm/s.

that the fundamental growth morphology can be derived from the morphological stability theory is broadly accepted [3,21,22]. This theory assumes that an initially planar front growing in z direction advancing at velocity V is perturbed with a spatial-time function $z = \delta \exp(\sigma t + \mathbf{i}2(\pi x/\lambda))$ where δ is the perturbation amplitude, λ is the wavelength and the growth rate of the perturbation σ can be determined from linear theory for small values of δ [6]. The solution for σ is a function which includes three terms: thermal, diffusive and capillary contributions:

$$\sigma = m_L G_C \xi_C - G - \frac{4\pi^2 T_m \Gamma}{\lambda^2} \quad (2)$$

Negative values of σ for all λ determine a stable planar front, positive values an unstable condition, and the particular case $\sigma = 0$ defines the marginal stability condition. In Eq. (2) G is the conductivity weighted temperature gradient defined by $G = [(\kappa_S G_S + \kappa_L G_L)/2\overline{\kappa}]$ where $\overline{\kappa} = (\kappa_S + \kappa_L)/2$ is the average of the solid and liquid conductivities. G_C is the composition gradient in the liquid, which for a planar interface at constant velocity is given by

$$G_C = \left[\frac{VC_0(k_0 - 1)}{k_0 D_L}\right] \quad (3)$$

Γ is the Gibbs-Thomson coefficient and ξ_C is a parameter given by

$$\xi_C = 1 + \frac{2k_0}{1 - 2k_0 - [1 + (4\pi D_L/v\lambda)^2]^{1/2}} \quad (4)$$

which is close to unity, except at rapid solidification conditions.

For a given growth velocity, between V_C (Modified Constitutional Supercooling) and V_{abs} (Absolute stability criterion), σ is positive for a range of wavelengths between λ_0^- an λ_0^+, defined where $\sigma = 0$ [22,6]. This zone has a value λ_{σ_M} where the planar growth will be unstable with a maximum perturbation rate σ_M. Fig. 4 shows this situation for a Al–0.2 wt.% Cu alloy growing at $V = 10^{-3}$ cm/s, following the proposal of Coriell and Boettinger [6].

Under the view of this linear theory, unstable growth would have a primary spacing determined by the contribution of a set of wavelengths, each characterized by a propagation rate σ. Discussion is open about how these wavelengths could contribute to the final spacing, but wavelengths close to λ_{σ_M} have greater probability to contribute to the primary spacing [3].

This fact could be seen superimposing experimentally measured spacings obtained for nodes, bands, regular and irregular cells on a stability map obtained for $G_L = 25$ K/cm and C_0= 0.2 wt.% Cu [6]. Fig. 5 shows that experimentally determined λ_1

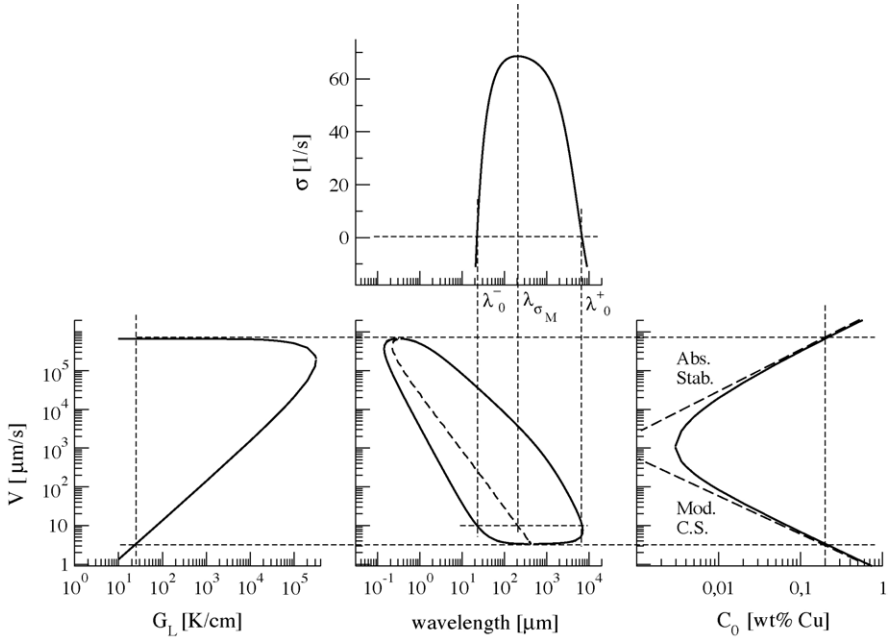

Fig. 4. Review of results of morphological stability theory for dilute Al–Cu alloys, after Coriell and Boettinger [6]. Remarked are the experimental conditions of this work. $C_0 = 0.2$ wt.% Cu; G_L =25 cm/s and an average velocity of $V = 10$ μm/s.

is found on the central part of unstable zone, close to wavelength for the maximum propagation rate. Similar results were obtained by Cheveigne et al. [23] in succinonitrile-acetone (transparent organic material). Also, Cheveigne et al. reviewed experimental results from different authors in metallic alloys with a similar tendency [24]. More recently, numerical predictions by Boettinger and Warren [25] in a 2D symmetry for intermediate and rapid growth velocities give the same behavior.

For these stages of growth, it was proved experimentally and numerically that the velocity of cells and dendritic tips of adjacent cells could be different [26,27]. In samples with low composition as our case, this differences in velocity could cause that the solute concentration of trapped intercellular liquid to be different so that some walls appear to contain eutectic $\alpha + \theta$ composition, while others do not. Consequently, low compositions promote irregular cellular structures. Under these conditions, it is necessary to reinterpretate the structures, taking into account that the final, lateral growth could happen in two different ways: in the presence or absence of eutectic composition in the intercellular space. In the former case, the cellular walls are simpler, with eutectic $\alpha + \theta$ composition. The low solute content implies that

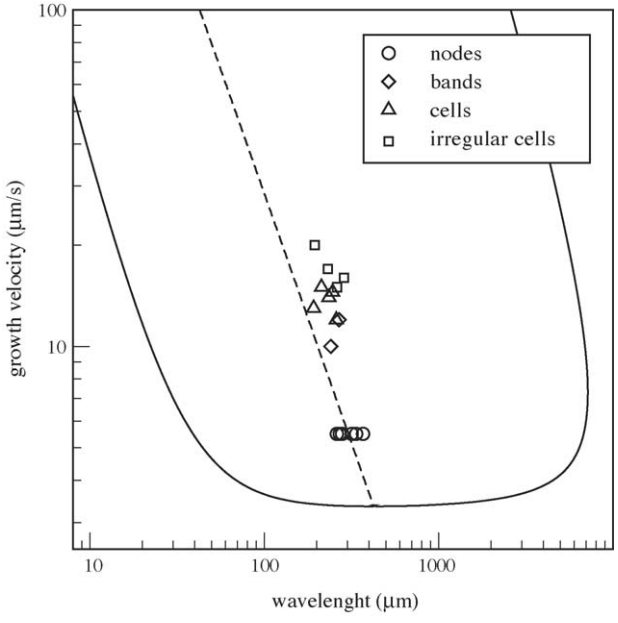

Fig. 5. Stability map of Al0.2 wt.%Cu, for $G_L = 25$ K/cm, superimposing λ_1 (open) and λ_{min} (closed symbols)

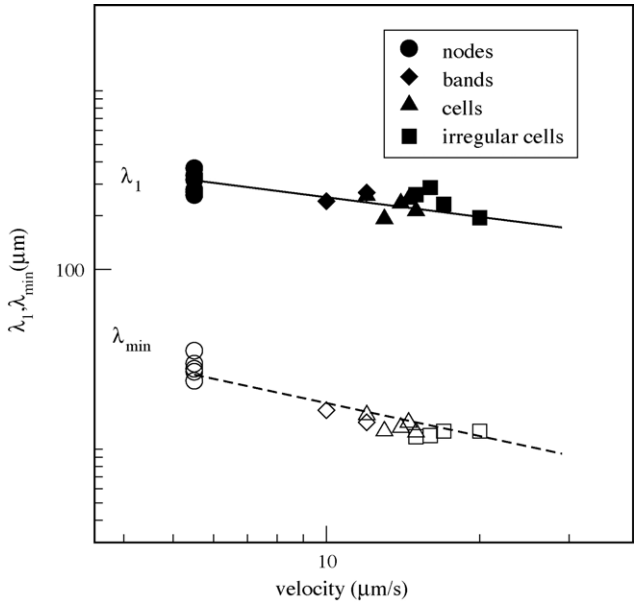

Fig. 6. λ_1 (open) and λ_{min} (closed symbols) vs. growth velocity.

the fraction of θ-phase would be low, but is enough to appear at a known spacing of approximately 10 μm, which is normal for Al–Cu eutectic directionally grown [28]. In the second case, we can find an enriched but not eutectic composition. The growth in this condition could be locally stable or unstable and apparently begin with the minimum unstable wavelength available in the system, close to the value of λ_0^-, although it may change with enough space and time to evolve [21]. In this way, it is possible to understand the behavior of the microstructure through the simplest concept of Constitutional Supercooling, a particular case of the stability theory at low values of V (see Fig. 4).

As it can be seen in the micrographs from Fig. 1 and 2, it is usual among nodes for a secondary level of segregation to appear, leaving in the sample a segregation pattern revealed by proper metallography. The pattern is characterized by a small perturbation during the final growth of two adjacent cells, trapping the last enriched liquid. The λ_{min} measured is significantly less than λ_1. In Fig. 6, λ_1 and λ_{min} as a function of the conditions in the solidification front are graphically represented. Notice that the slopes of both λ_1 and λ_{min} are similar, and λ_{min} is close numerically to the minimum wavelength that could be unstable, that is λ_0^-. This fact suggests that the primary spacing is formed funda-

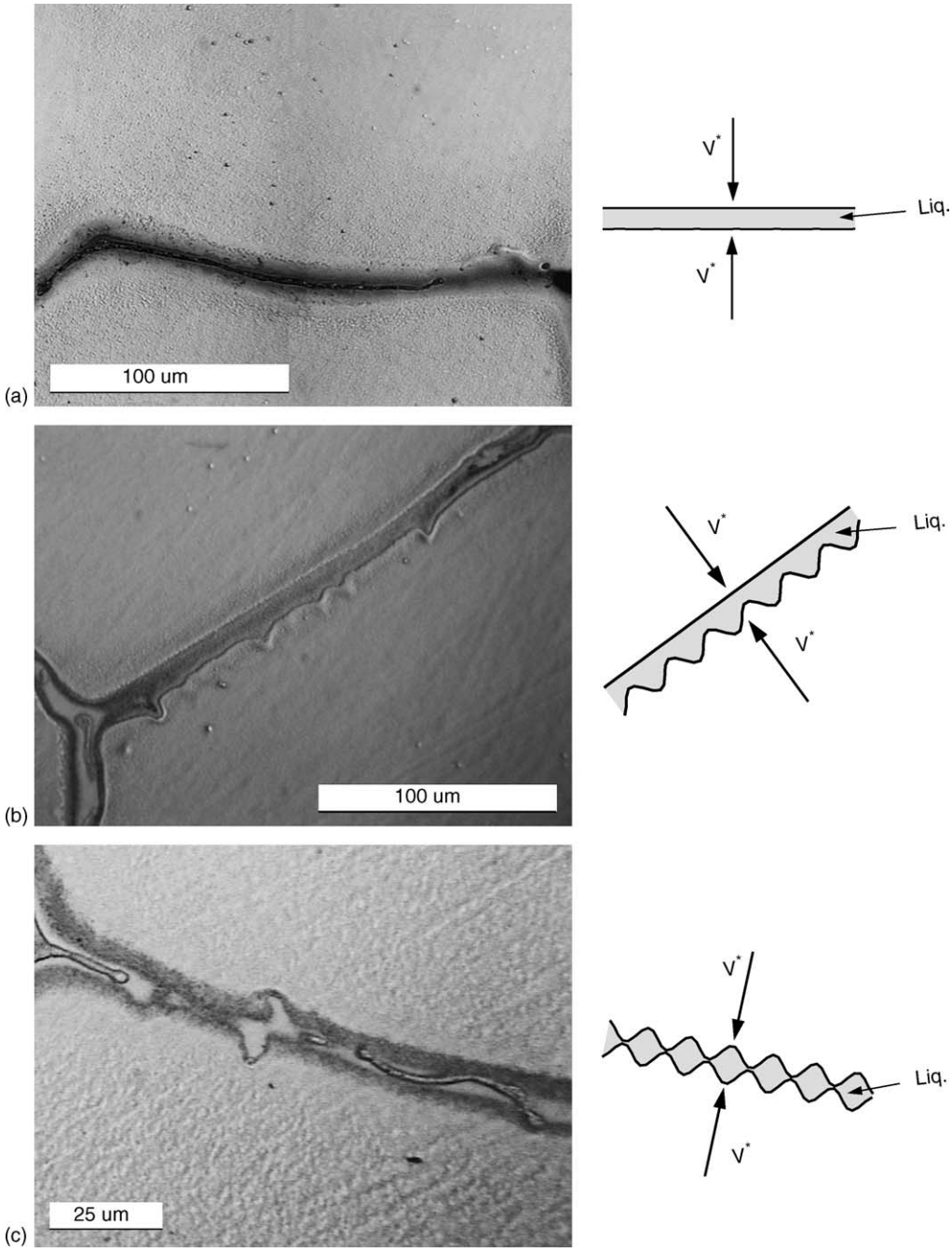

Fig. 7. Different cellular wall morphologies and a schematic interpretation of the microstructure: (a) lateral growth of two adjacent cells are stable; (b) lateral growth is unstable in one cell; (c) lateral growth in both cells is unstable.

mentally by wavelengths close to λ_{σ_M}, but with eutectic nodal precipitation, other wavelengths between λ_0^- and λ_{σ_M} can survive. It then seems logical to assume that once a eutectic node is formed, the lateral growth is driven by local solidification conditions, and as a consequence, it may be stable or unstable, depending on the local thermodynamical conditions affecting the local parameter (G_L/V^*C^*), where V^* and C^* are now the effective normal velocity and the effective concentration value at the local S–L interface. These different situations are metallographically detected as a planar segregation wall (if stable) or undulated segregation pattern (if unstable with $\lambda_{min} \sim \lambda_0^-$). Then different possibilities for the wall formation may be considered, as suggested in Fig. 7: (a) The lateral growth of two adjacent cells is stable, with a planar S–L interface: this case corresponds to a bidirectional growth where the interfaces confine an enriched liquid, which reaches the eutectic composition [9,6]. This situation concludes with a divorced continuous eutectic forming the wall, as can be seen in Fig. 7a. (b) Lateral growth is unstable in one cell: In this case, a regular segregated pattern appears, showing a planar interface form on one side and a perturbed interface on the other. This is shown in Fig. 1a and b and Fig. 7b, and it is the most common case found in the present experiments. (c) Lateral growth in both cells is unstable: given that small undulations of similar wavelengths appears from both sides. In this case it is possible to obtain divorced eutectic precipitation in local depressions of the interface. The origin may be a localized final solidification transient and or a solid precipitation during freezing of Cu enriched areas. This effect is related to the morphological characteristic of the solvus line of the Al–Cu alloy. Also, a continuous non planar eutectic wall could be found, as in Fig. 7c, with a final transient similar to the one discussed in the first point.

Then, under our experimental conditions, the evolution of the segregation substructure and the final segregation map for each stage and transitions from (i) to (v), seems to be a result of two superimposed growth mechanisms able to be explained qualitatively by the morphological stability theory. Thus, the evolution from stages (i) to (v) is a consequence of wavelengths of maximum propagation rate as predicted by the theory and the eutectic nodes fixed the local growth, conditioning the evolution of the substructure, while the minor instabilities λ_{min} associated to the microsegregation of the substructure walls are a result of the lateral solidification of the substructure, with a wavelength close to minimum unstable wavelength.

5. Conclusions

Al–0.2 wt.% Cu alloy samples were directionally solidified under similar thermal gradients. As the growth velocity was increased, the transition among successive stages appears, from planar, nodes, bidimensional cells, regular cells and irregular cells. These morphologies were characterized through careful metallographic analysis of the microsegregation. During the different transitions, a nodal mechanism seems to be responsible for the evolution of the substructure. The eutectic precipitation at nodes plays a fundamental role in the fixation effect of the substructure.

Particularly, during planar to bands transition, the nodes slow down the interface in certain critical points of it, and a spacing can be defined. This phenomenon seems to be similar during the transition of the all the substructure stages under study. This primary spacing (λ_1) fits the order of maximum rate wavelength predicted by the Morphological Stability Theory.

In several cases, a second order microsegregation pattern has been observed at level of the cellular walls, which seems to be due to a small variation in the microsegregation during the lateral growth of the cells in an enriched intercellular liquid. The microsegregation pattern detected has a wavelength that we call λ_{min}, and which is close to the minimum unstable wavelength predicted by the Morphological Stability Theory.

Acknowledgements

We wish to thank Dr. William Boettinger for useful comments. This work was performed at IFIMAT (Instituto de Física de Materiales Tandil) and was supported by CICPBA (Comisión de Investigaciones Científicas de la Provincia de Buenos Aires), CONICET (Consejo Nacional de Investigaciones Científicas y Técnicas), SeCAT-UNCPBA (Secretaría de Ciencia, Arte y Tecnología de la Universidad Nacional del Centro de la Provincia de Buenos Aires) and ANPCyT (Agencia Nacional de Promoción Científica y Tecnológica)

References

[1] R.F. Sekerka, Physica D 12 (1984) 212–214.
[2] S.R. Coriell, G.B. McFadden, R.F. Sekerka, J. Cryst. Growth 100 (1990) 459–466.
[3] S.R. Coriell, G.B. McFadden, Handbook of Crystal Growth, North Holland, 1993, pp. 785–857 (chapter 12: Morphological Stability).
[4] W.A. Tiller, K.A. Jackson, J.W. Rutter, B. Chalmers, Acta Metall. 1 (1953) 428–437.
[5] R. Trivedi, W. Kurz, Acta Metall. Mater. 42 (1994) 15–23.
[6] H. Biloni, W.J. Boettinger, R.W. Cahn, P. Haasen (Eds.), Physical Metallurgy, fourth ed., 1996, pp. 669–842 (chapter 8: Solidification).
[7] H. Biloni, R. di Bella, G.F. Bolling, Trans. Met. Soc. AIME 239 (1967) 2012.
[8] W.A. Tiller, J.W. Rutter, Can J. Phys. 34 (1956) 96.
[9] B. Chalmers, Principles of Solidification, Wiley and Sons, New York, 1964.
[10] W. Kurz, D.J. Fisher, Acta Metall. 29 (1981) 11–20.
[11] D.J. Wollkind, L.A. Segel, Phil. Trans. R. Soc. London A 268 (1970) 351–380.
[12] D.J. Wollkind, R. Sriranganathan, D.B. Oulton, Physica D 12 (1984) 215–240.
[13] B. Carolí, C. Carolí, B. Roulet, J. Cryst. Growth 76 (1986) 31–49.
[14] O. Fornaro, H.A. Palacio, Scripta Metall. Mater. 31 (1994) 1265–1270.
[15] O. Fornaro, H.A. Palacio, Scripta Mater. 36 (1997) 439–445.
[16] O. Fornaro, H.A. Palacio, H. Biloni, Mater. Res. Soc., 481 (1998) 21–26.
[17] O. Fornaro, H.A. Palacio, H. Biloni, Solidification Processes and Microstructures. A Symposium in Honor to Wilfried Kurz, The Minerals, Materials Society, (2004) 219–224.
[18] H. Biloni, G.F. Bolling, H.A. Domian, Trans. Met. Soc. AIME 233 (1965) 1926.
[19] M.C. Flemings, Solidification Processing, McGraw Hill, New York, 1974.
[20] A.P. Bond, G.F. Bolling, H.A. Domian, H. Biloni, J. Electrchem. Soc. 113 (1966) 773–778.
[21] Z. Bi, R.F. Sekerka, J. Cryst. Growth 237–239 (2002) 138–143.
[22] R. Trivedi, W. Kurz, Acta Metall. 34 (1986) 1663–1670.

[23] S. Cheveigné, C. Guthmann, M.M. Lebrun, J. Physique 47 (1986) 2095–2103.
[24] S. de Cheveigné, C. Guthmann, P. Kurowski, E. Vicente, H. Biloni, J. Cryst. Growth 92 (1988) 616–628.
[25] W.J. Boettinger, J.A. Warren, J. Cryst. Growth 200 (1999) 583–591.
[26] H. Son, S.N. Tewari, Metall. Matter. Trans. A 27 (1996) 1111–1119.
[27] M. Plapp, M. Dejmek, Europhys. Lett. 65 (2004) 276–282.
[28] W. Kurz, D. J. Fisher, Fundamentals of Solidification, third ed., Trans. Tech., 1989.